Available online at www.sciencedirect.com
SCIENCE DIRECT®
Journal of Contaminant Hydrology 82 (2006) 255–292
JOURNAL OF Contaminant Hydrology
www.elsevier.com/locate/jconhyd

Review article

Modeling and interpreting bioavailability of organic contaminant mixtures in subsurface environments

Nathan W. Haws *, William P. Ball, Edward J. Bouwer

Department of Geography and Environmental Engineering, Johns Hopkins University, 3400 N. Charles Street, Baltimore, MD 21218-2686, United States

Received 15 November 2004; received in revised form 29 September 2005; accepted 3 October 2005
Available online 28 November 2005

Abstract

Bioavailability often controls the fate of organic contaminants in surface and subsurface aquatic environments. Bioavailability can be limited by sorption, mass transfer, and intrinsic biodegradation potential and can be further altered by the presence of other compounds. This paper reviews current perspectives on the processes influencing subsurface contaminant bioavailability, how these processes are modeled, and how the relative role of the various processes can be assessed through bioavailability indices. Although these processes are increasingly well understood, the use of sophisticated models and indices often are precluded by an inability to estimate the many parameters that are associated with complex models. Nonetheless, the proper representation of sorption, mass transfer, biodegradation, and co-solute effects can be critical in predicting bio-attenuation. The influence of these processes on contaminant fate is illustrated with numerical simulations for the simultaneous degradation of toluene (growth substrate) and trichloroethylene (nongrowth cometabolite) in hypothetical, aerobic, solid–water systems. The results show how the relative impacts on contaminant fate of the model's various component processes depends upon system conditions, including co-solute concentrations. Slow biodegradation rates increase the inhibition effects of a cometabolite and suppress the rate enhancement effects of a growth substrate. Irrespective of co-solute effects, contaminant fate is less sensitive to biodegradation processes in systems with strong sorption and slow desorption rates. Bioavailability indices can be used to relate these findings and to help identify appropriate modeling simplifications. In general, however, there remains a need to redefine such indices in order that bioavailability concepts can be better incorporated into site characterization, remediation design, and regulatory oversight.
© 2005 Elsevier B.V. All rights reserved.

Keywords: Bioavailability; Sorption; Mass transfer; Biodegradation; Organic contaminants; Cometabolism

* Corresponding author. Tel.: +1 410 516 4255; fax: +1 410 516 8996.
E-mail address: nhaws@jhu.edu (N.W. Haws).

0169-7722/$ - see front matter © 2005 Elsevier B.V. All rights reserved.
doi:10.1016/j.jconhyd.2005.10.005

Contents

1. Introduction . . . 256
2. Processes that affect bioavailability: concepts . . . 257
3. Effects of solute mixtures on bioavailability. . . . 258
   3.1. Contaminant mixtures and soil–water partitioning . . . 258
   3.2. Contaminant mixtures and biodegradation . . . 259
   3.3. Contaminant mixtures and combined processes . . . 260
4. Processes that affect bioavailability: models. . . . 261
   4.1. Equilibrium sorption . . . 261
   4.2. Rate of mass transfer and desorption . . . 266
   4.3. Biodegradation . . . 270
5. Evaluation of bioavailability. . . . 271
6. Illustration of bioavailability concepts. . . . 275
   6.1. Model development . . . 275
   6.2. Parameterization . . . 276
   6.3. Results . . . 278
   6.4. Discussion . . . 281
7. Implications of bioavailability for field-scale bioremediation . . . 284
8. Conclusions . . . 285
Acknowledgements . . . 286
References . . . 286

1. Introduction

At sites where soils, sediments, and geologic media are contaminated with organic chemicals, in situ bioremediation and monitored natural attenuation are management options that can sometimes achieve acceptable levels of risk reduction at considerably less cost than ex situ or nonbiological alternatives such as pump and treat or continuous injection of chemical additives (NRC, 2003a). Even in cases where nonbiological techniques may be required to remove an imminent threat of contamination, in situ bioremediation or natural attenuation often will be a viable secondary strategy for site maintenance. Natural environments are complex, however, making it difficult to understand, identify, and characterize the underlying processes that control contaminant fate (Sturman et al., 1995; Alexander, 2000; Goltz et al., 2001; NRC, 2003a; Ehlers and Luthy, 2003).

The effectiveness of in situ bioremediation approaches (including natural attenuation) is often dictated by the ability of the native microbial population to take up and metabolize contaminants; however, observed rates of biodegradation in the field are often much lower than would be anticipated based solely on the results of laboratory studies with similar microbial populations and similar water/sediment mixtures (e.g., Rijnaarts et al., 1990; Scow and Hutson, 1992; Bosma et al., 1997; Alexander, 2000; Bogan and Sullivan, 2003; Ahmad et al., 2004). The decreased biodegradation rates in the field can be attributed to both spatial and temporal issues associated with upscaling from a simple batch system to a more complex subsurface domain. In a general sense, the problem arises from both differences in biological activity and decreased availability of the contaminants to microbes (i.e., bioavailability). Consequently, determining the bioavailability of substrates – and not only the intrinsic biodegradation potential – is an

important factor in estimating the feasibility of bioremediation at a site (Röling and van Verseveld, 2002).

Various definitions of bioavailability are used across many disciplines (NRC, 2003a; Madsen, in press; Semple et al., 2004). In this paper, the term bioavailability is applied in the context of the bio-attenuation of compounds found in the subsurface down gradient of a contamination source zone. The primary factors that influence bio-attenuation are sorption, mass transfer, and biological uptake (i.e., "bioavailability processes"; NRC, 2003a; Elhers and Luthy, 2003). Accurately predicting how each process influences contaminant removal is difficult, especially in systems with multiple contaminants (Baveye and Bladon, 1999; Madsen, in press). As a result, bioavailability concepts have yet to be well incorporated into site remediation tools and regulations.

To aid the interpretation and implementation of bioavailability principles, this paper reviews factors influencing contaminant bio-attenuation and the manner in which these factors have been conceptualized and modeled in recent literature. In addition, numerical simulations are conducted for hypothetical, aerobic, solid–water systems that are contaminated with toluene and trichloroethylene. The simulations exemplify the topics discussed in the paper, illustrate the manner in which specific combinations of the bio-attenuation processes can impact contaminant fate, and show how the relative importance of these processes are system dependent. Finally, this paper briefly discusses the need to more explicitly consider bioavailability in field site characterization, remediation design, and regulatory oversight.

2. Processes that affect bioavailability: concepts

In the context of bioremediation, contaminant bioavailability is commonly approached from the premise that chemicals are immediately accessible for microbial uptake only when in aqueous solution that is readily accessible to the advective flow of water—that is, the external aqueous phase of a solid–water batch system or the "mobile" phase of an advective system. The rationale behind this premise is that the small pore spaces (b 1 Am) internal to aggregates of soil and sediment particles exclude microbes, such that compounds that are dissolved or sorbed within these "immobile-water" domains must first be transported to the external aqueous phase (i.e., "bulk aqueous phase") before they can be metabolized (Steinberg et al., 1987; Bosma et al., 1997; Zhang et al., 1998; Ehlers and Luthy, 2003). This premise is supported by several laboratory studies that have found biodegradation to occur only, or predominantly, in the bulk aqueous phase (e.g., Ogram et al., 1985; Scow and Alexander, 1992; Smith et al., 1992; Zhao and Voice, 2000; Bengtsson and Carlsson, 2001). A few other studies have led researchers to conclude that at least some microorganisms are capable of degrading compounds directly from the sorbed phase (Guerin and Boyd, 1992; Tang et al., 1998; Feng et al., 2000). For many of these other studies, however, it is likely that the microbes did not actually metabolize compounds directly from the sorbed domain, but rather facilitated desorption by releasing surfactants or altering the subsurface redox conditions such that aqueous phase concentrations were increased (Alexander, 2000; NRC, 2003a, pp. 153–157 and references therein). Also, for many studies where solid-phase degradation was reported, biodegradation rates were nonetheless observed to decrease with contaminant soil–water contact time (Harms and Bosma, 1997; Alexander, 2000; Feng et al., 2000; Bogan and Sullivan, 2003; Ahmad et al., 2004). Overall, it appears that microbial access to contaminants is increasingly inhibited as solutes migrate deeper into submicron pores of impermeable sorption "domains" in soil–water environments.

If microbes only degrade solutes in the "mobile" aqueous phase, then rates of contaminant biodegradation will be reduced by sorption and/or diffusion into impermeable regions, with the

overall rate controlled by the slowest process of desorption or biotransformation (Scow and Hutson, 1992; Fry and Istok, 1994; Ghoshal et al., 1996; Bosma et al., 1997; Ramaswami and Luthy, 1997; Zhang et al., 1998; Braida et al., 2004). For example, in batch systems where the solids have a large sorption capacity, only a small fraction of the contaminant mass may be present in the bulk water. This can lead to a bfamine existenceQfor microbes, even in highly polluted environments (Bosma et al., 1997). Both numerical and batch experiments have shown that sorbent diffusion is often the limiting step, particularly in systems involving contaminants with large organic-carbon partition coefficients (K_{oc}) and large fine-pored aggregates with high organic matter content (Scow and Hutson, 1992; Fry and Istok, 1994; Bosma et al., 1997; Zhang et al., 1998; Shor et al., 2003; Sabbah et al., 2004). The rate-limiting step can also change over time. Using numerical simulations that considered diffusion, sorption, and biodegradation in a batch system, Scow and Hutson (1992) demonstrated that the shape of the biodegradation curve (% mineralized vs. time in aqueous concentration) can change from first-order toward zero-order over time, with the contaminants at first being rapidly degraded but slowing as intraparticle diffusion began to limit the replenishment of contaminant concentrations in the bulk aqueous phase. Scow and Alexander (1992) experimentally confirmed these numerical results using phenol and glutamic acid in a batch system with ceramic spheres.

Thus, bioavailability is influenced by a variety of factors, including physical characteristics of the sorbent (e.g., particle shapes, sizes, and internal porosities), chemical properties of the sorbates and sorbents, and biological factors (e.g., microbial abundance and affinity for the contaminant). These simultaneous processes coupled with field-scale complexities make in situ biodegradation rates difficult to isolate and verify by simply showing contaminant disappearance (Sturman et al., 1995; Odencrantz et al., 2003). Another important factor influencing bioavailability that is not as generally considered is the presence of other chemicals. Contamination at any site usually involves multiple contaminants that can compete for adsorption sites and for access to microbial enzymes. The potential impacts that the presence of co-solutes can have on bioavailability are discussed below.

3. Effects of solute mixtures on bioavailability

A contaminant's bioavailability can be influenced by the presence of other compounds. For example, co-solutes might compete for sorption sites, thereby increasing the aqueous concentrations and thus the overall bioavailability of a contaminant of interest. Conversely, they might decrease bioavailability by competing for microbial enzyme sites. This section reviews how the presence of co-solutes can affect bioavailability through altering one or more of the various processes that control overall degradation rates.

3.1. Contaminant mixtures and soil–water partitioning

The presence of multiple organic compounds results in increased competition for adsorption sites. As higher affinity adsorption regions become saturated by the competing solutes, the sorption of any given sorbate will be increasingly confined to lower affinity partitioning domains. This usually linearizes the single-solute sorption isotherms and reduces the sorption affinity for the less strongly sorbed solutes (McGinley et al., 1993, 1996; Schaefer et al., 2000; Xia and Ball, 2000; Graber and Borisover, 2003). The extent of the competition and isotherm linearization with co-contamination will depend on the sorbent material. Materials such as hard carbon, for which surface adsorption is dominant, will exhibit more competitive effects than

bsoftQorganic matter, for which non-competitive absorption dominates partitioning (McGinley et al., 1996; Allen-King et al., 2002). The degree of co-solute effects on sorption will, of course, also depend on the specific chemicals involved. For example, co-solutes with similar molecular functionality will usually have affinity for similar sorption sites and will show increased competitive effects (e.g., Xing et al., 1996; Xing and Pignatello, 1998; Li and Werth, 2001; Graber and Borisover, 2003).

An exception to this general trend was documented by Martins and Mermoud (1998). These researchers measured sorption isotherms for four nitroaromatic herbicides. All compounds exhibited linear isotherms in the single-solute systems, but in the mixed system, the sorption isotherm of all the herbicides, except 2,4 dinitrophenol (DNP), became strongly nonlinear ($n = 0.55$ to 0.7). The authors reasoned that DNP preferentially filled most of the available strong adsorption sites such that the competitive effects of DNP left only a sparse distribution of weak adsorption sites that led to nonlinear isotherm behavior for the other solutes. This situation is unusual, however, because high affinity adsorption sites will commonly be less abundant.

As an example of competitive sorption causing less retardation, Rivett and Allen-King (2003) observed that the advective transport of PCE at the Borden research site was approximately 3 times greater in a DNAPL dissolution experiment than in an earlier study where solute separation had occurred (e.g., Curtis et al., 1986; MacKay et al., 1986) and that the apparent sorption of PCE was more linear than in the prior study. In the more recent study, the source area concentrations of PCE and other competing solutes (TCE, TCM) were nearly 4000 times greater than in the prior experiment, and the researchers hypothesized that these higher concentrations caused increased competition and decreased solute retardation. This hypothesis was supported by batch sorption studies with single and mixed solutes.

Experiments have also verified that co-solute competition can increase intrasorbent diffusion rates. For example, White and Pignatello (1999) showed that desorption rates for phenanthrene increased in the presence of greater pyrene concentrations. They reasoned that the faster desorption rates were caused by the competing solutes blocking some of the soil micropores and/or swelling the organic matter, thus permitting the phenanthrene to move more rapidly through the intraparticle regions of the soil particles. A similar effect has been reported by Allen-King et al. (2002). They demonstrated that the sorption-based retardation of diffusion in a clay aquitard at Sarnia, Ontario, was less at higher concentrations, and in a manner that was consistent with the known nonlinearity of the solute's isotherm (in this case the saturation of high affinity sorption sites was caused by the solute itself). Such concentration-based and competitive sorption effects on desorption rates would be expected for retarded intragranular diffusion in any impermeable zone where competitive sorption occurs.

3.2. Contaminant mixtures and biodegradation

Excluding effects related to microbial growth (which are discussed subsequently), the presence of multiple substrates will generally reduce the intrinsic (aqueous) biodegradation rates of the individual compounds. This binhibitionQresults from more substrate molecules vying for the active enzyme sites. For homologous substrates (compounds with similar catabolic pathways), inhibition is typically competitive – that is, one substrate binds to an enzyme to form an enzyme–substrate complex that blocks another substrate from forming a complex with that enzyme – but noncompetitive or uncompetitive inhibition are also possible. Noncompetitive inhibition occurs when two compounds independently bind to the same enzyme, which decreases the overall utilization rate. Uncompetitive inhibition is similar to noncompetitive

inhibition except that the second substrate (the inhibitor) can bind to an enzyme complex with the first substrate but not to a free enzyme (Copeland, 1996; Reardon et al., 2000; Alvarez-Cohen and Speitel, 2001).

Even with co-solute inhibition, the biodegradation rates for some compounds may increase because of accelerated biomass growth on multiple substrates. For example, Guha et al. (1999) observed that, in a mixed system of naphthalene, phenanthrene, and pyrene, the mineralization rate of the more readily degradable naphthalene slowed, yet the biodegradation rates of more recalcitrant phenanthrene and pyrene were enhanced. The slower naphthalene transformation rate resulted from competitive inhibition while the enhanced rates of the other PAHs were attributed to greater biomass growth.

Enhanced biodegradation rates in co-solute systems can also occur when the solute of interest does not function as a growth substrate. This process, cometabolism, occurs when a growth substrate induces microbes to produce enzymes that bfortuitouslyQ degrade a nongrowth substrate, even though the nongrowth substrate provides little or no growth or energy benefit to the microbes (Criddle, 1993; Semprini, 1997; Alvarez-Cohen and Speitel, 2001). Cometabolism is particularly important in the bioremediation of some otherwise recalcitrant contaminants. Examples of environmentally relevant compounds that have been observed to cometabolically biodegrade include trichloroethylene (TCE), dichloroethylene (DCE) and vinyl chloride (VC) in the presence of aromatic degraders (Schafer and Bouwer, 2000; Alvarez-Cohen and Speitel, 2001; Gandhi et al., 2002; Shingleton et al., 2001; Meza et al., 2003) and methanogenic cultures (e.g., Alvarez-Cohen and Speitel, 2001; Kim et al., 2002); chloroform in the presence of aromatic degraders and methanogens (Gupta et al., 1996; Hamamura et al., 1997); and MTBE in the presence of alkane degraders (Dupasquier et al., 2002; Magar et al., 2002; Smith et al., 2003). Although cometabolism enhances biotransformation of some compounds, the degradation rates for cometabolites are typically slow and subject to inhibition by the primary substrate. For example, the aerobic cometabolic degradation rate of TCE is often observed to be less than an order of magnitude of that of the biodegradation rates of the corresponding growth substrates (Arp et al., 2001).

In addition to the primary substrate effects on cometabolite degradation, cometabolites may suppress the biodegradation rate of the growth substrate through competitive inhibition and due to increased biomass decay rates that may result from toxic effects of cometabolic transformation products (Semprini, 1997; Alvarez-Cohen and Speitel, 2001; Arp et al., 2001). These potential negative impacts necessitate a careful balance between growth substrate and cometabolite concentrations to ensure continued biodegradation at a site.

3.3. Contaminant mixtures and combined processes

Co-solute effects on individual bio-attenuation processes will not necessarily couple through a simple linear superposition of the various processes as modeled in isolation. Interactions of co-solutes with the media, microbes, and other solutes blikely translate into non-linear effects in scalingQand b[as] a consequence, processes need to be understood within the complexity of their natural states.Q(NRC, 2003a, pp. 198–199). One example of how the bioavailability constraints imposed by one process can modify the significance of co-solute effects on another process is from the study of the four nitroaromatic compounds by Martins and Mermoud (1998) that was cited earlier. In this study, the researchers monitored the biodegradation of the nitroaromatics in liquid, batches (water with soil suspensions) and in unsaturated solid, batches (repacked soils). They observed that 2, 4-dinitrophenol (DNP) and 2-methyl-4, 6-dinitrophenol (DNOC) were

rapidly biotransformed in the single-solute, liquid batches, but that the transformation rates were significantly reduced when these compounds were combined with 2-*sec*-butyl-4, 6-dinitrophenol (DNSB) and 2-*tert*-butyl-4, 6-dinitrophenol (DNTB) due to inhibition and toxicity effects. Conversely, in the solid batches, the multi-solute degradation rates were actually greater than the single-solute rates. The researchers reasoned that greater mass transfer constraints in the solid batches lowered the contaminant-microbe contact and consequently reduced toxicity.

To better predict contaminant fate in single- and multi-solute environments, modeling approaches need to accurately account for the individual and combined effects of the biotic and abiotic processes. The following section reviews traditional and more recent approaches for modeling the sub-component processes that affect bioavailability.

4. Processes that affect bioavailability: models

4.1. Equilibrium sorption

Sorption collectively describes *adsorption* of solutes onto particle surfaces and *absorption* (*partitioning*) of solutes into macromolecular organic phases (Luthy et al., 1997; Allen-King et al., 2002; Huang et al., 2003). Distinguishing between adsorption and absorption mechanisms is difficult, and inferences of microscale sorbate–sorbent interactions are often made through macroscale observations of sorption isotherm characteristics (Luthy et al., 1997; Xia and Pignatello, 2001; Madsen, in press). Isotherm nonlinearity is typically bfavorableQ (higher sorbed-to-aqueous ratios at low aqueous concentrations) and is often most pronounced at low aqueous concentrations. At higher concentrations, the higher energy sorption sites become saturated, absorption into bsoftQ organic matter becomes the dominant sorption mechanism, and the isotherm becomes more linear (Xia and Ball, 1999; Xia and Pignatello, 2001; Huang et al., 2003).

Properly delineating the sorption isotherm over the entire concentration range of interest is important because misrepresenting nonlinear sorption behavior with a linear sorption isotherm can lead to overestimations of contaminant bioavailability at low solute concentrations (e.g., Karapanagioti et al., 2001; Sabbah et al., 2004). In addition, separately understanding what fraction of sorption is due to linear partitioning and what fraction is associated with nonlinear processes can also be important because only the latter tend to be competitive (e.g., Xia and Ball, 1999, 2000; Huang et al., 2003). In this context, recently observed sorption isotherms with soils and sediment have been represented as combinations of both linear and nonlinear sorption mechanisms, as more fully reviewed by Allen-King et al. (2002). These dual-mode, combined sorption, or composite models (Weber et al., 1992; Xing et al., 1996; Huang et al., 1997; Xia and Ball, 1999, Huang et al., 2003) have demonstrated particular strength in representing sorption behavior of organic solutes to mixed carbon sources such as sediments or soils that are composed of both natural organic matter and combustion residues or other forms of thermally altered carbon (Allen-King et al., 2002; Huang et al., 2003; Cornelissen and Gustafsson, 2004). The disadvantage of composite models, however, is the increased number of fitting parameters that complicate the estimation of unique parameter sets (Allen-King et al., 2002; Li and Werth, 2002).

Common sorption isotherms for the nonlinear (adsorption) component are shown in Table 1. (See Hinz, 2001 for a good review of mathematical isotherm expressions.) The *Freundlich* isotherm model (Eq. (B), Table 1) is perhaps the most widely applied model to describe nonlinear sorption behavior. The observed n values are less than one for sorption onto most

Table 1
Some equilibrium sorption isotherm models commonly applied for soils and sediments

Name	Equation	Parameters	Example References
Linear	$S = K_d C$ [A]	C = aqueous-phase equilibrium concentration [$M_c\ L_w^{-3}$] S = sorbed-phase equilibrium concentration [$M_c\ M_s^{-1}$] K_d = sorption partition coefficient [$L_w^3\ M_s^{-1}$]	Karickhoff et al. (1979)
Freundlich	$S = K_f C^n$ [B]	K_f = Freundlich sorption coefficient [$(L_w^3\ M_s^{-1})^n$] n = Freundlich exponent [–]	Freundlich (1932) Do (1998) Hinz (2001)
Langmuir	$S = \frac{S^{max} b C}{1 + bC}$ [C]	S^{max} = maximum sorption capacity [$M_c\ M_s^{-1}$], b = sorption affinity parameter [–]	Langmuir (1918) Do (1998) Hinz (2001)
Polanyi–Dubinin–Manes	$S_m = S_m^{max} \rho_o \exp\left[\frac{\varepsilon_{sw}}{E}\right]^b$ [D.1]	ρ_o = density of the compound [ML^{-3}] ε_{sw} = available adsorption potential = $RT\ln(C_{sol}/C_e)$ [$L^2\ T^{-2}$] C_{sol} = aqueous solubility of compound [ML^{-3}] C_e = equilibrium solute concentration [ML^{-3}] R = ideal gas constant [$L^2\ T^{-2}$], T = absolute temperature [Kelvin]	Crittenden et al. (1987) Sontheimer et al. (1988) Manes (1998) Kleineidam et al. (2002) Allen-King et al. (2002)
	$S_m = S_m^{max} \rho_o \mathrm{dl0\hat{}}c\left[\frac{\varepsilon_{sw}}{NF}\right]^b$ [D.2]	c = fitting parameter [–] E = normalization factor = E_ob [$L^2\ T^{-2}$] E_o = reference free energy of adsorption [$L^2\ T^{-2}$] b = sorption affinity coefficient [–] NF = normalization factor, often taken to be V_s V_s = bulk molar volume of the adsorbate at the temperature of adsorption [$L^3\ M^{-1}$]	
	note: $S_m = \frac{S}{V_s}$		
Multi-component Langmuir	$S_i = \frac{S_i^{max} b_i C_i}{1 + \sum_{j=1}^{N} b_j C_j}$ [E]	i = solute i (solute of interest) j = solute j N = number of solutes in system	Markham and Benton (1931) Do (1998) Li and Werth (2002)
Ideal Adsorbed Solution Theory (IAST)	$C_i = \frac{S_i}{\sum_{j=1}^{N} S_j} \left[\frac{n_i}{K_{fi}} \sum_{j=1}^{N} \frac{S_j}{n_j}\right]^{\frac{1}{n_i}}$ [F]		Radke and Prausnitz (1972) Crittenden et al. (1985) McGinley et al. (1993, 1996) Schaefer et al. (2000) Li and Werth (2002)

sorbents from aqueous solution, indicating the gradual filling of higher energy sorption sites as concentration increases. Although n values are usually only slightly less than one for soils and sediments, recent studies on hard carbon materials, such as combustion residues, have reported n values of 0.6 or less (Kleineidam et al., 2002; Huang et al., 2003; Cornelissen and Gustafsson, 2004; Cornelissen et al., 2004a,b; Nguyen et al., 2005).

Another, useful sorption model is based on the *Polanyi–Manes* (PM) approach (Manes, 1998; Crittenden et al., 1987; Sontheimer et al., 1988), which, when applied in the form of the Dubinin–Astakov equation, has been referred to as the *Polanyi–Dubinin–Manes* (PDM) model (Allen-King et al., 2002; Kleineidam et al., 2002). The Dubinin–Astakov equation (or PDM) is shown as Eqs. (D1) and (D2) of Table 1. The PM approach is based on Polanyi's theory of adsorption potential for a vapor phase system (Allen-King et al., 2002), and can also be applied to aqueous systems based on theory described elsewhere (Wohleber and Manes, 1971a,b; Manes, 1998). The basic assumption of the PM approach is that the available sorption potential, ε_{sw}, decreases as the adsorbed concentration increases—i.e., during filling of micropores in the adsorption domain. The PM approach is particularly suited for situations where the volume available for sorbed molecules is not a function of temperature and is constant for multiple sorbates (Manes, 1998), but the underlying theory is generally applicable to any adsorption process. It is important to recognize that the PM approach does not specify any particular relation between the adsorbed volume and ε_{sw}, such that Eq. (D1) (or equivalently (D2)) is only one convenient mathematical formulation (Manes, 1998).

As previously mentioned, competitive sorption adds complexity to predicting sorbent–water interactions. There are several methods to account for changes in the equilibrium distribution of one solute when in the presence of other sorbates. For example, the single solute Langmuir isotherm is easily extended to a multi-component Langmuir isotherm (Table 1, Eq. (E)). Similar to its single component counterpart, the multi-component Langmuir model assumes a fixed number of sorption sites and no interactions among sorbates (Li and Werth, 2002).

The PDM model also can be modified to account for multiple sorbates by assuming that the adsorbed solution is ideal (or, that the equilibrium sorbed phase activity of an individual solute is proportional to its mole fraction in the sorbed solution; i.e., Raoult's Law), that the adsorption potential of each solute is the same at equilibrium, and that the total sorption potential of the mixture is the same as the potential of a single sorbate with the same adsorbed volume as the mixture. Modifications of the theory that assume other, less ideal, mixtures of solutes are also available (Manes, 1998). With the ideal solution assumption, the definition of the available sorption potential for the PM approach can be modified for a solute i in a mixture of n components according to the following equations (Xia and Ball, 2000; Li and Werth, 2002):

$$\varepsilon_{sw\ i} \quad RT \ln \left[x \frac{C_s}{C} \right]_i \tag{1a}$$

$$x_i \quad \frac{C_i}{C_i^*} \tag{1b}$$

$$\sum_{i\ 1}^{n} x_i \quad 1 \tag{1c}$$

where C_s is the solubility of the solute and C_i* is the aqueous concentration of solute i with the same adsorbed volume as the total adsorbed volume of the mixture at equilibrium.

Table 2
Intraparticle mass transfer and sorption/desorption rate models

Name	Equation	Parameters	Example References
Spherical intraparticle diffusion with surface diffusion to the bulk aqueous phase	$\frac{B}{Bt}\,e_{im}C_{im}\,r \quad qS\,r$ $\frac{1}{r^2}\frac{B}{Br}\,e_{im}D_p r^2\frac{BC_{im}}{Br}$ [A.1] where: $C_{im}(r=a)=C_a$ and $\frac{BC_b}{Bt} \quad \frac{3dV_s}{adV_w}a_s\,C_a \quad C_b \quad e_I D_p \frac{BC_{im}}{Br}_{r\ a}$ [A.2]	C_{im}=aqueous phase solute concentration in intraparticle region [ML ^{3}] C_a=aqueous phase solute concentration at particle surface [ML ^{3}] C_b=bulk aqueous solute concentration [ML ^{3}] D_p=effective pore diffusion coefficient [L^2 T ^{1}] V_s=unit soil volume [L^3] V_w=unit water volume [L^3] r=particle radial coordinate [L] a=radial position the particle surface [L] q=soil bulk density [ML ^{3}] $_{im}$=intraparticle porosity [–] a_s=surface mass transfer coefficient [LT ^{1}]	Crank (1975) Rao et al. (1980a) Crittenden et al. (1986) Miller and Pedit (1992)
First-order mass transfer	$\frac{BC_b}{Bt} \quad a_p\,C_{im} \quad C_b$ [B]	a_p=first-order mass transfer coefficient [T ^{1}]	van Genuchten and Wierenga (1976) van Genuchten et al. (1977a,b)
One-site desorption	$\frac{BS}{Bt} \quad k_d S \quad \frac{k_a}{R_{s\,w}}C$ [C.1] $\frac{BS}{Bt} \quad k_d\,K_d C \quad S$ [C.2]	C=aqueous phase concentration [ML ^{3}] S=sorbed phase concentration [MM ^{1}] $R_{s/w}$=soil/water ratio [ML ^{3}] k_a=first-order sorption rate [T ^{1}] k_d=first-order desorption rate [T ^{1}] $K_d \quad \frac{dS}{dC}g \quad \frac{k_a}{R_{s\,w}dk_d}$	Oddson et al. (1970) Lindstrom et al. (1971)
Two-site desorption (fast/instantaneous+slow)	$\frac{BS_r}{Bt} \quad fK_d\frac{BC}{Bt}$ [D.1] $\frac{BS_s}{Bt} \quad k_s \quad 1 \quad f \quad K_d C \quad S_s$ [D.2] $\frac{S\ t}{S_o} \quad 1 \quad f \quad \exp \quad k_s t$ $f \quad \exp \quad k_r t$ [D.3]	S_o=initial sorbed phase concentration [MM ^{1}] f=fraction of rapid/instantaneous sorption sites [–] k_s=desorption rate for slow sorption sites [T ^{1}]	Brusseau et al. (1989) Gamerdinger et al. (1990) Cornelissen et al. (1997)

Table 2 (*continued*)

Name	Equation	Parameters	Example References
Two-site desorption (fast/instantaneous+slow) Three-site sorption	$\frac{\partial S_{k_i}}{\partial t} = k_i f_{k_i} K C - S_{k_i}$ [E.1] $\frac{S(t)}{S_o} = f_r \exp(-k_r t) + f_s \exp(-k_r t) + (1 - f_r - f_s)\exp(-k_{vs} t)$ [E.2]	k_r=desorption rate for rapid sorption sites [T^{-1}] f_r=fraction of rapid sorption sites [–] f_s=fraction of slow sorption sites [–] f_{vs}=fraction of very slow sorption sites [–] k_{vs}=desorption rate for very slow kinetic domain [T^{-1}]	Johnson et al. (2001) Pedit and Miller (1994) ten Hulscher et al. (1999) Johnson et al. (2001)
Continuum-site sorption (e.g., gamma distribution)	$\frac{\partial S_{k_i}}{\partial t} = \int_k k f_k K C - S_k \, dk$ [F.1] $\frac{S(t)}{S_o} = 1 - \left(\frac{\beta}{\beta + t}\right)^{\gamma}$ [F.2]	γ, β=gamma distribution parameters for the probability, f, of a domain with desorption rate, k: $f(k) = \frac{\beta^{\gamma} k^{\gamma-1} \exp(-\beta k)}{\Gamma(\gamma)}$ $\Gamma(\gamma) = \int_0^{\infty} x^{\gamma-1} \exp(-x) \, dx$	Connaughton et al. (1993) Ahn et al. (1996) Culver et al. (1997) Sahoo and Smith (1997) Johnson et al. (2001)

The sorption model most commonly used to predict adsorption isotherms for solutes in mixtures is derived from the *ideal adsorbed solution theory* (Crittenden et al., 1985; McGinley et al., 1993; Xing et al., 1996; Schaefer et al., 2000; Li and Werth, 2002), which was originally developed for vapor-phase adsorption and later applied to liquid solute systems by Radke and Prausnitz (1972). The main assumptions of the IAST are similar to those of the ideal solution in the PM approach; that is, that solutes in a multi-component system have access to the same sorption sites and that Raoult's Law applies. Also similar to the competitive PM approach, the IAST assumes that the total spreading pressure – the isothermal difference in interfacial tension between the pure solvent–solid and solution–solid interface – is equivalent for the single- and the multi-solute systems under conditions of equal activity in solution at any given temperature (Xing et al., 1996; Porter et al., 1999). Then, the equilibrium aqueous concentration of each solute in the mixture is equal to the concentration it would have in a single-solute system with the same spreading pressure as in the mixture. An important aspect of both the PM and IAST approaches is that sorption isotherms for multi-component systems can be constructed based on their single-solute isotherms. Eq. (F) of Table 1 shows the IAST equation for the aqueous concentration of a solute i in a multi-component system based on Freundlich isotherms for the individual solutes.

The IAST has been effectively used to predict multi-solute sorption for numerous sorbents with a variety of organic compounds (e.g., McGinley et al., 1993, 1996; Xing et al., 1996); however, the approach has been less successful predicting competitive sorption in some other cases involving heterogeneous sorption domains (Schaefer et al., 2000; Xing et al., 1996). In addition, multi-component sorption models based on IAST are generally less accurate at high

solute concentrations and in mixtures with significant solute–solute interactions, where assumptions of ideality are violated (Porter et al., 1999; Li and Werth, 2002). Thus, challenges remain in developing a robust model for simulating sorption behavior in mixed systems across a wide concentration range and with a wide variety of sorbents.

4.2. Rate of mass transfer and desorption

A prominent conceptualization of mass transfer ascribes rate limitations as the physical process of slow diffusion of solutes through intraparticle pores or other intrasorbent regions (Wu and Gschwend, 1986; Brusseau et al., 1989; Ball and Roberts, 1991b). This process is conceptually distinct from sorption–desorption dynamics, a chemical phase-partitioning to solid phases. As both mechanisms affect the rate at which solute mass becomes available in the aqueous phase, however, they can be difficult to distinguish in natural environments. For this reason, and because models of both processes are often mathematically analogous, they are discussed together here.

Several different models are commonly used to describe mass transfer and phase-partitioning rates in environmental systems. Solute mass transfer within a soil or sediment particle is typically thought of as a Fickian diffusion process, assuming, for example, an appropriate average size of spherical particles and radially symmetric transport (see Table 2, Eq (A.1)). In cases where only aqueous pore diffusion is allowed (i.e., sorbed or surface diffusion is negligible or nonexistent), rates of change in the total sorbed concentration will be retarded by sorption along the pore of the intrasorbent diffusion domain. Solute diffusion within a particle is driven by the concentration boundary condition, $C(r=a)=C_a$, which, in turn, is controlled by the solute concentration in the bulk aqueous phase (C_b) and an external surface diffusion (Table 2, Eq. (A.2)). In many environmental applications of this approach, the characteristic time for surface diffusion is taken to be much less than the characteristic time for intraparticle mass transfer, such that surface diffusion can be safely neglected and $C_a=C_b$.

In contrast to the uniform sphere assumptions, however, actual solids have heterogeneous sizes, geometries, and internal porosities. Nonetheless, there has been some success in modeling solute mass transfer, or sorption and desorption, by estimating an average spherical diffusion (or sorption–desorption) rate constant and also allowing a fraction of more rapidly (essentially instantaneous) equilibrating sites to exist (e.g., Rao et al., 1980a,b; Addiscott et al., 1983; Nkedi-Kizza et al., 1983; Ball and Roberts, 1991b; Young and Ball, 1994). Other, more recent, investigations have explicitly considered multiple particles sizes, each with its characteristic diffusion rate (Kleineidam et al., 1999; Karapanagioti et al., 2001; Başağaoğlu et al., 2002) and, as will be described subsequently, distributions of rates corresponding to multiple diffusion conditions.

Because definitive characteristics of sorbent physical and chemical characteristics are usually unattainable, and also to simplify the mathematics of modeling, the intraparticle mass transfer is frequently reduced to a first-order rate of solute exchange between mobile and immobile regions (Table 2, Eq. (B)). The first-order mass transfer coefficient is an acknowledged approximation which can never be mechanistically correct, and several investigators have described how the first-order rate must vary over time to simulate a Fickian diffusion process (Rao et al., 1980a; Young and Ball, 1995; Griffioen et al., 1998; Maraqa, 2001). In general, first-order rate models are rarely able to accurately simulate solute concentration histories in either batch or column studies (Young and Ball, 1997; Griffioen, 1998); however, if multiple first-order rate coefficients

are allowed to exist (Table 2, Eqs. C, D, and E) and/or if other system properties (such as the sorption capacity or column dispersivity) are simultaneously fit to experimental data, then reasonable simulations of observed data can sometimes be obtained. Parameter values obtained from such fits, however, should be regarded as case-specific, with little to no direct link to any mechanistic processes of mass transfer.

Another model of desorption rates is based on chemical kinetics under a set of presumed conditions that would cause the rate of desorption to be proportional to the concentration difference between the aqueous and sorbed phases (Table 2, Eq. (C)). Though conceptually distinct, this is mathematically identical to the first-order mass transfer model (Nkedi-Kizza et al., 1984) and, as with the other first-order approaches, two or more first-order rate coefficients are often used to describe desorption/diffusion kinetics from heterogeneous sorbents (Table 2, Eqs. (D)–(E)).

Another well-developed approach for modeling mass transfer and sorption/desorption rates in real soils and sediments is to assume the existence of a diverse distribution of rate constants that are described by a probability density function (pdf). Perhaps the most commonly applied pdf approach, shown in Eq. (F) of Table 2, uses the gamma pdf to simulate a continuum of sorption/desorption rates or diffusion domains (Connaughton et al., 1993; Ahn et al., 1996; Culver et al., 1997; Sahoo and Smith, 1997); although other distribution functions, such as the lognormal density function, have also been applied (Pedit and Miller, 1995; Haggerty and Gorelick, 1998; Li and Brusseau, 2000; Zhang and Brusseau, 2004). Using the gamma distribution model, Culver et al. (1997) achieved significant improvement over the more traditional two-site model in describing long-term desorption behavior for batch and pulse-input column experiments. The rate distribution parameters, however, were sensitive to flow conditions in column experiments and varied between batch and column experiments. A comparison by Johnson et al. (2001) of the gamma distribution model with five other two- or three-compartment desorption models found that the gamma distribution model accurately fit phenanthrene desorption profiles for some soils (Lachine shale and a sandy soil with shale particles accounting for most of the organic matter), but it had difficulty predicting desorption from geologically younger topsoil. They concluded that a two- or three-site model could fit their desorption data as well as or better than the gamma distribution model, argued that the parameters for a two- or three-site model are easier to interpret, and recommended applying a two-site model based on radial diffusion as the best desorption model with three or fewer fitting parameters. Overall, however, this and numerous other studies make it clear that no simply parameterized model can be mechanistically correct for heterogeneous materials of unknown composition, and that any choice of model must be used cautiously with regard to predictions outside of its range of calibration.

As noted previously, because the first-order approach is unable to capture the internal particle solute dynamics, the rate bconstantsQ often need to vary with the experimental time and conditions in order to accurately simulate results (Rao et al., 1980a; Young and Ball, 1995, 1997; Griffioen, 1998; Maraqa, 2001; Haggerty et al., 2004). Moreover, potential errors associated with using a first-order rate model to describe nonequilibrium kinetics are often not apparent from short-term experiments despite the fact that these errors can be substantial over longer times. Generally, good predictions should not be expected for boundary conditions, initial conditions, or time frames different than those with which the first-order parameter was specifically calibrated (Rao et al., 1980a; Young and Ball, 1995; Sabbah et al., 2004). In addition, because a first-order rate cannot capture the intraparticle dynamics during cyclic mass transfer (such as when desorption is onset before sorption is complete), models using first-order

Table 3
Biodegradation models based on Monod kinetics

Name	Equation	Parameters	Example References
Monod Equation (Michaelis–Menten)	$r_g \quad \frac{dC_g}{dt} \quad \frac{q_{mg} X C_g}{K_{sg} \quad C_g}$ [A.1]	K_s=half-velocity constant (the aqueous substrate concentration when the growth rate is at one-half of its maximum value) [M_g/L^3]	Monod (1949)
		X=concentration of microorganisms [M_x/L^3]	Tchobanoglous and Burton (1991)
		Y=maximum yield coefficient (mass of microbial cells formed per mass of contaminant substrate consumed) [$M_x\ M_g^{-1}$]	Alvarez-Cohen and Speitel (2001)
	$r_x \quad \frac{dX}{dt} \quad \mu_{mg} X \quad Y r_g \quad bX$ [A.2]	b=microbial endogenous decay coefficient [T^{-1}]	
		$q_{mg}=\mu_{mg}/Y_g$ [$M_g\ M_x^{-1}\ T^{-1}$]	
		r_g=growth substrate utilization rate [$M_g\ L^{-3}\ T^{-1}$]	
		r_x=rate of microbial cell growth [$M_x\ L^{-3}\ T^{-1}$]	
		μ_m=maximum specific growth rate [T^{-1}]	
First-order	$r_s \quad q_1 C_s$ [B]	q_1=first-order biodegradation rate coefficient [T^{-1}]	
Zero-order	$r_s \quad q_0$ [C]	q_0=zero-order biodegradation rate coefficient [$ML^{-3}\ T^{-1}$]	
Competitive inhibition	$r_g \quad \frac{q_{mg} X C_g}{K_{sg} \quad 1 \quad \sum_{j\ 1}^{n} \frac{C_c}{K_{ic}^C} \quad C_g}$ [D]	K_{ic}^C=competitive inhibition coefficient [ML^{-3}]	Criddle (1993)
		n=number of cometabolites in system	Alvarez-Cohen (1993)
			Copeland (1996)
			Reardon et al. (2000)
			Alvarez-Cohen and Speitel (2001)
Noncompetitive inhibition	$r_g \quad \frac{q_{mg} X C_g}{K_{sg} \quad C_g \quad 1 \quad \sum_{j\ 1}^{n} \frac{C_c}{K_{ic}^N}}$ [E]	K_{ic}^N=noncompetitive inhibition coefficient [ML^{-3}]	Keenan et al. (1994)
			Copeland (1996)
			Reardon et al. (2000)
			Alvarez-Cohen and Speitel (2001)
Uncompetitive inhibition	$r_g \quad \frac{q_{mg} X C_g}{K_{sg} \quad C_g \quad 1 \quad \sum_{j\ 1}^{n} \frac{C_c}{K_{ic}^U}}$ [F]	K_{ic}^U=uncompetitive inhibition coefficient [ML^{-3}]	Copeland (1996)
			Reardon et al. (2000)

Cometabolic degradation	$r_c \quad T_y r_g \quad q_{mc} X \quad \frac{C_c}{K_{sc} \quad C_c}$ [G]	T_y=transformation yield (ratio of the mass of cometabolic substrate transformed to the mass of growth substrate transformed) [M_c M_g ^{1}] r_c=rate of cometabolic nongrowth substrate utilization [M_g L ^{3} T ^{1}]	Alvarez-Cohen and McCarty (1991a,b) Criddle (1993) Alvarez-Cohen and Speitel (2001) Ely et al. (1995) Alvarez-Cohen and Speitel (2001)
Cometabolic degradation with product toxicity	$q^4_{mg} \quad q_{mg} \quad q_{inact} P_c \quad q_{rec} P_g$ [H.1] $q^4_{mc} \quad q_{mg} \; q_{mg} \quad q_{inact} P_c \quad q_{rec} P_g \; q_{mg}$ [H.2] $r_x \quad Y r_g \quad bX \quad \frac{r_c}{T_c}$ [I]	P_g=product of the growth substrate [M/L^3] P_c=product of the cometabolic substrate [M/L^3] T_c=transformation capacity=$\frac{C_c}{X}$ [M_c $M_{x\ 1}$] q_{mg}*=modified maximum utilization rate for growth substrate [T ^{1}] q_{inact}=first-order cell inactivation rate [T ^{1}] q_{rec}=first-order cell recovery rate [T ^{1}]	
Reductant limitation	$r_g \quad q_{mg} X \quad \frac{C_g}{K_{sg} \quad C_g} \quad \mathrm{d} \quad \frac{C_r}{K_{sr} \quad C_r}$ [J.1] $r_r \quad a_g \quad r_g \quad a_c \quad r_c$ [J.2]	C_r=aqueous concentration of reductant [M/L^3] K_e=half-velocity constant for reductant [ML ^{3}] a_c=stoichiometric coefficient for reductant consumption from biodegradation of cometabolic substrate [M_r M_c ^{1}] a_g=stoichiometric coefficient for reductant regeneration from biodegradation of growth substrate [M_r M_g ^{1}]	Chang and Alvarez-Cohen (1995) Alvarez-Cohen and Speitel (2001)
Haldane–Andrews self-inhibition model	$r_g \quad \frac{q_{mg} X C_g}{K_{sg} \quad C_g \quad C_g \quad \frac{C_g}{K_i}^{\ n}}$ [K]	K_i=inhibition coefficient [–] n=order of inhibition (n=1 for traditional Haldene–Andrews equation)	Edwards (1970) Neufield et al. (1980) Gupta et al. (1996)

rates can erroneously predict desorption (and inaccurately imply desorption hysteresis) under such conditions (Griffioen, 1998; Sabbah et al., 2004).

4.3. Biodegradation

Biodegradation models (Table 3) are commonly based on saturation kinetics (Monod, 1949; Copeland, 1996; Kovárová-Kovar and Egli, 1998). The classical Monod expression (Table 3, Eqs. (A.1), (A.2)) models the interdependence of the degradation of a rate-limiting substrate and the biomass growth as functions of a yield coefficient Y [$M_x M_g^{-1}$] (biomass formed per mass of contaminant substrate consumed) and a maximum specific microbial growth rate, μ_m [T^{-1}]. (Often μ_m and Y are lumped into a single maximum rate of substrate utilization, q_m [$M_g M_x^{-1} T^{-1}$]). The rate of substrate utilization and biomass growth are influenced by a half-velocity constant, K_s [ML^{-3}], which conceptually represents the affinity of the degrading enzyme for the substrate (Copeland, 1996; Kovárová-Kovar and Egli, 1998). When the microbial culture is in the log-growth phase, the biomass growth is reduced by a first-order endogenous decay rate coefficient, b [T^{-1}] (Tchobanoglous and Burton, 1991; Kovárová-Kovar and Egli, 1998).

The Haldane–Andrews equation (Table 3, Eq. (K)) modifies the original Monod equation to account for when a substrate (or substrate biotransformation intermediate) is toxic to the degrading population. The effects of this "self-inhibition" are incorporated into the Monod expression with an inhibition term, C/K_i [–] in the denominator. The Haldane–Andrews equation is similar to the Monod equation at low substrate concentrations, but gives decreased utilization rates as the substrate concentration is increased. A modified form of the Haldane–Andrews equation adds an exponent n (the order of reaction) to the inhibition term (Gupta et al., 1996).

Further variations to the Monod equation account for co-solute effects, including reductant limitations, co-solute inhibition, and cometabolism with product toxicity. These modifications for co-solutes are shown in Eqs. (D)–(J) of Table 3. (See Copeland, 1996 for a more comprehensive review of models for co-substrate inhibition or Alvarez-Cohen and Speitel, 2001 for a review of these models in the context of cometabolism). Theoretically, the inhibition term, K_i, in the inhibition models (Table 3, Eqs. (D)–(F)) is equivalent to the half-velocity constant, K_s, for that compound (Copeland, 1996). As discussed in Reardon et al. (2000) and Alvarez-Cohen and Speitel (2001), however, this substitution often fails to capture the complexities of intracellular solute interactions, and, consequently, a more nondescript inhibition term is often empirically determined.

A challenge in applying any form of the Monod equation is determining appropriate kinetic parameters. Reported values of μ_m and K_s vary by as much as 3 orders of magnitude, even for the same combination of substrate and microbial culture (Kovárová-Kovar and Egli, 1998). Likely reasons for parameter variations are correlations between μ_m and K_s, the history and condition of the degrading population, and experimental data quality and regression technique (Kovárová-Kovar and Egli, 1998). Thus, although there have been a variety of studies to measure μ_m, K_s, and other parameters, the general applicability of their values is unclear, especially for multi-substrate Monod models that require several additional parameters (Semprini, 1997; Alvarez-Cohen and Speitel, 2001). Consequently, for reasons similar to the use of first-order rate models for mass transfer (i.e., inability to characterize the system and/or for mathematical simplicity), the Monod expression is often reduced to a single rate constant. Making this simplification requires the assumption of zero net biomass growth ($r_x = 0$). Then, if the solute concentration is much less than the half-velocity constant ($C \ll K_s$) the Monod equation for substrate degradation reduces to a

first-order equation with a rate constant, $q_1 = q_{mg} X K_{sg}^{-1}$ [T^{-1}] (Table 3, Eq. (B)), or, if $C \ll K_s$, the Monod equation becomes zero-order with rate constant, $q_0 = q_{mg} X$ [$ML^{-3}T^{-1}$] (Table 3, Eq. (C)). In modeling solute attenuation in many laboratory experiments and contaminated field sites, a first-order biodegradation rate is the de facto representation, justified by aqueous solute concentrations that are typically low relative to their respective K_s values (Bjerg et al., 1996). In many cases, the use of a first-order biodegradation rate constant may be necessary because it is infeasible to separate all the biological processes affecting biodegradation in a way needed to parameterize the Monod model. As with the use of a first-order mass transfer constant, however, it should be recognized that an empirically determined first-order biodegradation rate constant is site specific and subject to variations in experimental conditions (including, and especially, when in the presence of co-solutes), and temporal variations in the biomass population. Slight modifications to the first-order approximation, such as including an initial "lag" period of no degradation, can sometimes improve the ability of a first-order model to account for nonideal processes such as microbial adaptation (e.g., Zimdahl et al., 1994; Martins and Mermoud, 1998; Park et al., 2001, 2002). Still, the applicability of a first-order rate model for long-term predictions is hard to validate and should not be extended beyond the specific situation under which it was determined.

5. Evaluation of bioavailability

Bioavailability is often evaluated using dimensionless indices that provide a simple measure of the relative magnitude of mass transfer rates to biodegradation rates with the idea that exceptionally high or low values can provide an indication of the rate limiting mechanism. Table 4 summarizes bioavailability indices used in prior research. For example, one such index is the Damköhler number, χ, defined as the ratio of the first-order biodegradation rate coefficient to either an overall first-order mass transfer rate coefficient (Table 4, Eq. (A.1)) or an external surface (film) mass transfer coefficient (Table 4, Eq. (A.3)). The Bioavailability Number of Bosma et al. (1997) is the reciprocal of χ with the Monod parameters K_s and l_m used to approximate a first-order biodegradation rate coefficient (Table 4, Eq. (B)). Another bioavailability index, the Thiele Modulus, ϕ_T, is the square root of the ratio of the biodegradation rate to the diffusion/desorption rate (Table 4, Eqs. (C.1)–(C.3)). The Thiele Modulus is also used to account for mass transfer rate effects in the Bioavailability Factor of Zhang et al. (1998), which also accounts for effect of equilibrium sorption and the soil–water ratio on the overall rate of biodegradation (Table 4, Eq. (D)).

By identifying the process limiting mass removal, bioavailability indices can assist in the design of remediation strategies. For example, sites with a high bioavailability index (biodegradation rates ≫ mass transfer rates) are likely amenable to bioremediation while sites with a low bioavailability index might require treatments that act to increase aqueous concentrations of the contaminants such as thermal or cosolvent flushing (Zhang et al., 1998).

The utility of a bioavailability index depends on the degree that a value calculated from independently obtained data can reveal the remediation potential at a given site and the ease with which new data can be obtained to adjust the value for new site conditions. This interpretability and transferability will, in turn, depend on the extent to which discernable mechanistic aspects of bioavailability are captured by the index and on whether the assumptions about their interrelations are valid. In this regard, one limitation of bioavailability indices is that, as single dimensionless coefficients, they only convey relative rates and not the absolute rates for mass transfer and biodegradation. Consequently, a simple bioavailability index alone does not

Table 4
Dimensionless bioavailability indices used in prior research

Name	Equation	Parameters	Example references
Damköhler number (χ)	$\chi \quad \frac{q_1}{a}$ [A.1] or $\chi \quad \frac{q_1}{n v_p A_p k_f}$ [A.2]	A_p=surface area per unit volume of a single particle [L ^{1}] q_1=first-order biodegradation rate constant [T ^{1}] a=the first-order mass transfer rate constant [T ^{1}] n=number of particles [–] v_p=volume of a single particle [L^3] k_f=surface mass transfer coefficient [LT ^{1}]	Ghoshal et al. (1996) Ramaswami and Luthy (1997) Chung et al. (1993)
Bioavailability number (B_n)	$B_n \quad \frac{a K_s}{\mu_m} \frac{1}{\chi}$ [B]	K_s=Monod half-velocity constant [ML ^{3}] μ_m=Monod maximum utilization rate [T ^{1}]	Bosma et al. (1997)
Thiele Modulus (Φ_T)	$\Phi_T \quad \frac{a}{3} \quad \frac{q_1}{D_a}^{\frac{1}{2}}$ [C.1] or $\Phi_T \quad a \quad \frac{\theta_{im} \quad R \; 1 \quad \theta_{im} \; q_1}{D_a}^{\frac{1}{2}}$ [C.2] or $\Phi_T \quad \frac{q_1}{k_2 K_d R_{s\,w}}^{\frac{1}{2}}$ [C.3]	D_a=effective interparticle diffusion coefficient (D_p/R) [L^2 T ^{1}] K_d=linear soil–water partition coefficient [L^{3}M ^{1}] R=retardation factor [–] $R_{s/w}$=soil–water ratio [ML ^{3}] a=particle radius [L] k_2=first-order desorption rate constant q_1=first-order biodegradation rate coefficient [T ^{1}] θ_{im}=intraparticle porosity [–]	Myrold and Tiedje (1985) Chung et al. (1993) Zhang et al. (1998)
Bioavailability factor (B_f)	$B_f \quad \frac{1}{1 \quad K_d R_{s\,w} \quad 1 \quad \frac{q_1}{k_2 K R_{s\,w}}}$ [D]		Zhang et al. (1998)

distinguish a situation where biodegradation and mass transfer rates are mutually rapid from a situation where biodegradation and mass transfer rates are similarly slow (both situations could theoretically have the same bioavailability index).

In the latter regard, it is useful to consider a two-dimensional plot of the mass transfer rate, r_{mt}, versus the biodegradation rate, r_{bio}, as shown in Fig. 1. Such a plot displays both the absolute and relative rates for r_{mt} and r_{bio}. It also allows a quick assessment of both the limiting processes as well as the overall remediation potential of a site. For example, contaminated sites where the plot of r_{mt} vs. r_{bio} lies in regions of the graph near $r_{bio}=0$ (extreme biodegradation rate limitations) or $r_{mt}=0$ (extreme mass transfer rate limitations) are not good candidates for in situ bioremediation or natural attenuation, and the remediation potential increases toward the upper right portion of

Fig. 1. Two-dimensional depiction of a bioavailability index, BI=r_{mt}/r_{bio} (r_{mt}=mass transfer rate and r_{bio}=biodegradation rate.). Contaminated sites where BI plots near $r_{bio}=0$ (extreme biodegradation rate limitations) or $r_{mt}=0$ (extreme mass transfer rate limitations) are not good candidates for bioremediation or natural attenuation. The feasibility of bioremediation and natural attenuation increases toward the upper right portion of the graph. The numbered arrows represent potential co-solute effects (see Table 5 for explanation).

the graph. A slightly different graphical approach for quantifying bioavailability, recently presented by Braida et al. (2004), was based not directly on rates but rather on the basis of specific experimental endpoints that could be obtained in the laboratory. Although the axis and quadrants of their graph were less clearly defined, the experimental approaches were designed to independently estimate biodegradation rates and thereby isolate mass transfer effects. Generally, such approaches are likely needed to classify sites on the basis of bioavailability.

The interpretability and transferability of bioavailability indices is dependent on the approximations used in their development. Current indices are based on mathematical relationships that are derived from equations for a completely mixed, batch system with homogeneous, spherical solids and rely on simplistic representations of both biodegradation and mass transfer. Also, the current bioavailability indices do not explicitly show the effects of the possible presence of other chemicals. As has been discussed throughout this paper, co-solutes can either increase or decrease mass transfer rates and biodegradation rates—see the numbered arrows in Fig. 1 and the corresponding explanations in Table 5. Consequently, before a bioavailability index can be applied to a given situation, it is important that the index be modified to account for the other solutes in the system. A similar ambiguity in interpreting the current bioavailability indices is that it is unclear how the index incorporates the effects of equilibrium sorption. Because sorption lowers a solute's aqueous concentration, it will reduce the apparent biodegradation rate. Also, stronger sorption in intraparticle regions will reduce apparent mass transfer rates. Consequently, before a bioavailability index can be correctly interpreted for a given site or transferred from one compound to another, it should be understood whether the biodegradation and mass transfer rates used in the index calculation were measured in the presence of sorption or if they reflect intrinsic rates as would be observed in a system with no sorption.

A further limitation of any bioavailability index is that it can only relate information for a single-time point in the site history. The bioavailability at a site, however, likely changes over

Table 5
Possible co-solute effects on bioavailability

No.	Co-solute effect on bioavailability	Parameters
1	Increased r_{mt}: competitive sorption reduces retardation. Unchanged r_{bio}: biomass growth is at steady-state and the biodegradation rate is a zero-order process (high substrate concentration). No cometabolic, inhibitive, or toxicity effects.	Sorption n b 1 Biodegradation K_s b C K_i H C T_c Y I
2	Unchanged r_{mt}: noncompetitive sorption Increased r_{bio}: increased biomass and or cometabolism outweigh any toxic or inhibitive effects.	Sorption n = 1 Biodegradation T_c Y I T_y N0
3	Unchanged r_{mt}: noncompetitive sorption Decreased r_{bio}: toxic and/or inhibitive effects outweigh biomass growth or cometabolic effects.	Sorption n = 1 Biodegradation K_i b C T_c Y 0
4	Increased r_{mt}: as in case (1) Increased r_{bio}: as in case (2)	Sorption n b 1 Biodegradation T_c Y I T_y N0
5	Increased r_{mt}: as in case (1) Decreased r_{bio}: as in case (3)	Sorption n b 1 Biodegradation K_i b C T_c Y 0

The numbered scenarios correspond to the numbered arrows shown in Fig. 1. The last column indicates likely values of the principal sorption and biodegradation parameters for the given scenario. (r_{mt} = mass transfer rate and r_{bio} = biodegradation rate).

time. For example, Monod biodegradation kinetics will fluctuate with time depending on changes in both the aqueous solute concentrations and the growth or decay of biomass. Likewise, mass transfer rates will decrease over time as concentration gradients within immobile zones decrease, and this trend will be magnified in materials with nonlinear sorption isotherms. The dependence of mass transfer rates on the solute distribution makes even a single-time bioavailability index difficult to estimate at a site if the prior system history and initial contaminant profiles within the immobile zones are unknown.

It is uncertain whether site and process characterization can ever be sufficient to allow the development of more robust bioavailability indices that account for site-specific conditions of sorption equilibrium, mass transfer rates, biodegradation kinetics, initial spatial distributions of contaminants, and solution chemistry. This does not mean, however, that simpler bioavailability indices can be of no practical value. Rather, a bioavailability index can aid in site characterization and remediation if the time and condition-specific nature of the indicators is appropriately acknowledged. For example, time varying bioavailability indices could be used as part of an adaptive management approach that includes both initial field-scale testing and periodic recalibration of indices over time based on occasional field-scale perturbations and measurements (NRC, 2003b). The potential usefulness and limitations of bioavailability indices can be illustrated through some specific example calculations based on numerical simulations in

a well defined batch system. Such simulations and associated discussions are provided in the remaining sections of this paper. Additional exemplary calculations and alternative methods of rate comparison (to directly illustrate effects from the variability of biodegradation rates over time) are provided elsewhere (Haws et al., in press).

6. Illustration of bioavailability concepts

To illustrate how co-solute and mass transfer constraints influence contaminant bioavailability, numerical simulations were conducted for hypothetical cases studies of the fate of a primary growth substrate (toluene) and a cometabolically degraded non-growth substrate (trichloroethylene) in single and dual substrate systems. Toluene and trichloroethylene (TCE) were chosen because of their environmental relevance as both individual contaminants and as cometabolic substrates and because of the availability of reported aerobic biodegradation parameters for these compounds.

6.1. Model development

The numerical model used in this work incorporates fully reversible and linear sorption and simple, lumped mass transfer/desorption with Monod biodegradation kinetics for solutes in a well-mixed batch system of a water-saturated sorbent. The forward and reverse mass transfer is represented by a one-site sorption domain:

$$C \underset{k_d}{\overset{k_a}{\rightleftharpoons}} S$$

where C [ML ^{3}] is the aqueous-phase solute concentration, S [MM ^{1}] is the sorbed-phase concentration, and k_a and k_d [T ^{1}] are the respective first-order sorption and desorption rate constants. Accordingly, the equilibrium soil–water partitioning coefficient, K_d [L^{3}M ^{1}], for a given soil–water ratio, $R_{s/w}$ [ML ^{3}], is defined by the following equation:

$$K_d \quad \frac{k_a}{R_{s\ w} k_d} \qquad 2$$

The linear sorption model does not include competitive sorption effects and assumes that an effective intraparticle diffusion rate parameter can be lumped into the sorption and desorption rate coefficients. Though certainly not realistic for actual soil/sediment systems, this representation is useful to explore some of the basic processes that influence bioavailability and to establish some baseline cases against which other, more complex, modeling results might be compared. Similarly, the well-mixed batch conditions are not realistic for most environmental systems but can be considered to represent an endpoint of behavior that might be observed in the laboratory or under certain special cases of controlled remediation.

Single component biodegradation is modeled using the Monod expressions given in Eqs. (A.1)–(A.2) of Table 3. Co-contaminant inhibition is incorporated with the competitive inhibition representation given by Eq. (D) of Table 3. Cometabolism and product toxicity are simulated using Eqs. (G) and (I) of Table 3. Nutrients and energy substrates are assumed to be non-limiting.

The numerical solution for coupling mass transfer and biodegradation was programmed using MS Excel/Visual Basic. Aqueous and sorbed concentrations, as well as the microbial growth or decay, were updated at each time step using a central-weighted, finite-difference scheme. The

numerical algorithm first solved for the contaminant distribution between aqueous and sorbed phases, and then used this result to calculate the mass of substrate degraded and the change in the biomass concentration.

6.2. Parameterization

All case studies were for a 1 L, completely mixed, aerobic batch domain with $R_{s/w}$=4.4. This $R_{s/w}$ corresponds to the solid and water ratios that would exist in saturated aquifers with soil bulk densities, q, in the range of 1.5 to 1.9 g/cm^3 and water contents, h, in the range of 0.34 to 0.43. Two hypothetical soils were investigated. The first, a weaker sorbent (Type I), was representative of aquifer sands in Borden, Ontario with an organic carbon fraction of 0.00023 (D' Adamo, 2003). The second, a stronger sorbent (Type II), was typical of silt loam aquitard material in Dover, Delaware with an organic carbon fraction of 0.015 (D' Adamo, 2003). Although sorption in the Borden material has been found to be slightly nonlinear and in excess of that estimated from typical correlations with organic matter (Ball and Roberts, 1991a; Rivett and Allen-King, 2003; Ran et al., 2003), the simulations in this work for both Borden and Dover materials are simplified to be based on linear partition coefficients, K_d, that were estimated from partition coefficients, K_{oc}, normalized to the fraction of organic carbon, f_{oc}:

$$K_d \quad f_{oc}K_{oc} \qquad 3$$

The K_{oc} values were approximated from reported octanol–water partition coefficients, K_{ow}, with the relationship used by Schaerlaekens et al. (1999) and based on the long-standing correlation of Karickhoff (1981):

$$\log K_{oc} \quad 0\ 95 \log K_{ow} \quad 0\ 2 \qquad 4$$

As recently reviewed by Allen-King et al. (2002), this correlation is but one of many empirical correlations that give similar results to within approximately 0.3 to 1.0 log units for various nonpolar organic chemicals. Recently published equations (see Allen-King et al., 2002) provide more accurate techniques to estimate sorption strength. Correlations of K_{oc} with K_{ow} are still in common use, however, and Eq. (3) is sufficient for the illustrative purposes of this work.

First-order desorption rate coefficients, k_d, were approximated from the computed K_d values using the regression relationship of Brusseau et al. (1991):

$$\log k_d \quad 0\ 7 \log K_d \quad 1\ 67 \qquad 5$$

As with Eq. (4), the k_d K_d regression in Eq. (5), is used here for simplicity and as a crude means of approximating a first-order constant that includes some of the effects of increased retardation and slowed mass transfer that are expected to occur under conditions of diffusion-limited desorption with intraparticle sorption (Ball et al., 1991).

The specific log K_{ow} value for TCE, 2.32, was taken from the averages of several literature values assembled by Schaerlaekens et al. (1999). The log K_{oc} value for toluene, 2.18, was obtained directly from values reported by E.P.A. (1995). The K_d and k_d values used in each simulation are reported in Table 6.

Selecting representative values for the aerobic biodegradation parameters of each contaminant was difficult because of the large number of parameters and the large variation of reported values within a given parameter class (see Section 4.3). However, toluene and/or TCE biodegradation parameter values compiled by Semprini (1997), Alvarez-Cohen and Speitel (2001), Alagappan and Cowan (2003), Arp et al. (2001), as well as other individual studies (see

Table 6
Equilibrium sorption partition coefficients (K_d) and first-order desorption rate coefficients (k_d) used in the simulations with the Borden-like solids (Type I) and the Dover-like solids (Type II)

	Toluene	TCE
Type I soil		
K_d (L kg $^{-1}$)	0.035	0.024
k_a (d $^{-1}$)	0.83	0.77
k_d (d $^{-1}$)	5.4	7.3
Type II soil		
K_d (L kg $^{-1}$)	2.2	1.6
k_a (d $^{-1}$)	2.8	2.7
k_d (d $^{-1}$)	0.29	0.39

footnotes to Table 7) provided a suitable dataset from which to estimate average biodegradation parameter values. TCE biodegradation parameters were taken only from experiments of TCE cometabolism where toluene or phenol was used as the primary growth substrate.

The reported biodegradation rates from studies using pure-strain microbial cultures were generally greater than those reported for studies using mixed microbial cultures. To highlight the effects of biodegradation rate, two biodegradation parameter sets were compiled for toluene and TCE: one using average values from the pure culture studies (termed bfastQ) and one using average values from the mixed culture studies (termed bslowQ). The value of the bfastQ K_s was also used for both the bfastQ and bslowQ K_i values. (Recall that the validity of substituting K_s values for K_i values is still under debate; however, a lack of reported K_i values necessitated this assumption.) For each simulation, the initial biomass concentration, X, was set at 5 mg/l, which is within the range of reported values for batch biodegradation studies (McCarty et al., 1998; Schafer and Bouwer, 2000; Alagappan and Cowan, 2003; Kim et al., 2002).

To show the effects of the initial contaminant concentrations, two different scenarios of initial contaminant mass were also explored: one at a higher initial contaminant mass (high M_o) and one at a lower initial mass (low M_o). For TCE, the high M_o was 100 Amol and the low M_o was 1 Amol. The M_o for toluene was set at 10 times the M_o for TCE. The M_o values were selected to provide initial high/low concentrations that bounded typical values used in biodegradation studies and bioremediation scenarios (McCarty et al., 1998; Cupples et al., 2004; Schafer and Bouwer, 2000; Alvarez-Cohen and Speitel, 2001). The initial solute distributions between

Table 7
Aerobic biodegradation parameters used for bfastQ and bslowQ biodegradation rates

	Toluene[a]		TCE[b]	
	Fast (pure cultures)	Slow (mixed cultures)	Fast (pure cultures)	Slow (mixed cultures)
q_m (Amol mg_x^{-1} d^{-1})	200	130	8	2
K_s (mol L^{-1})	30	100	10	30
K_i (Amol L^{-1})	30	30	10	10
Y (mg_x Amol $^{-1}$)	0.05	0.03	n.a.	n.a.
T_y (Amol Amol $^{-1}$)	n.a.	n.a.	0.09	0.05
T_c (Amol mg_x^{-1})	n.a.	n.a.	0.25	0.25

[a] Average of values reported in Chen et al. (1992), Chang and Alvarez-Cohen (1995), Semprini (1997), Arp et al. (2001), Alagappan and Cowan (2003), Kim et al. (2004).
[b] Average of values reported in El-Farhan et al. (1998), Chang and Alvarez-Cohen (1995), Semprini (1997), Alvarez-Cohen and Speitel (2001), Arp et al. (2001).

aqueous and sorbed phases were set to the equilibrium value for the given $R_{s/w}$ and K_d. In order to evaluate the effects of co-solutes, additional simulations were also conducted for systems with only a single component, toluene or TCE, at high and low M_o.

The different scenarios for the Type I and Type II soils, the fast and slow biodegradation parameters, the high and low M_o values, and the single and dual solute scenarios combined for a total of 16 simulations. Fig. 2 shows the conditions assumed for the various scenarios and provides identification numbers for cross-reference use in subsequent figures.

6.3. Results

The relative mass remaining (M/M_o) for toluene and TCE is plotted against time for each simulation in Figs. 3 and 4, respectively. Because toluene has consistently greater relative mass reduction than TCE, a semi-log scale is used in Fig. 3 and a linear scale is used in Fig. 4. For the dual contaminant system with the bfastQbiodegradation parameters, toluene degradation is fairly

Fig. 2. Outline of scenarios for simulations of toluene and TCE biodegradation. M_o refers to the initial mass of toluene or TCE in the batch system.

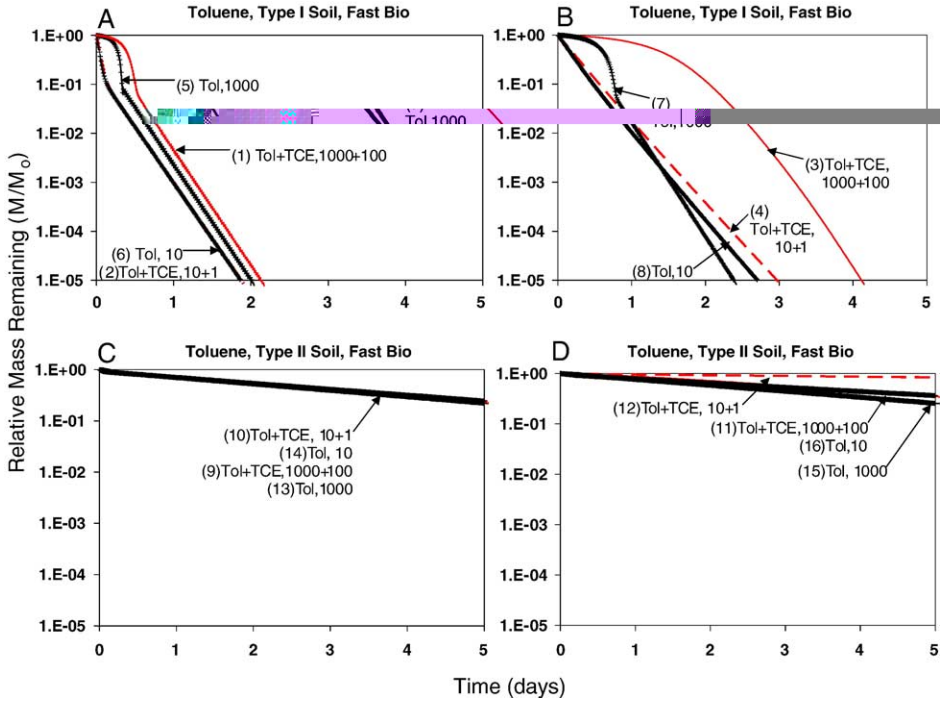

Fig. 3. Relative mass remaining for toluene for the various soil-type, concentration, biodegradation parameters, and single substrate (Tol) vs. dual substrate (Tol+TCE) scenarios.

insensitive to the presence of TCE (Fig. 3A and C). There is no perceptible difference between the toluene degradation in the dual contaminant scenario and the toluene-only scenario for the low M_o cases; however, for the high M_o case in the Type I soil, the presence of TCE noticeably inhibits toluene degradation.

In contrast to toluene, the mass removal of TCE in the TCE-only scenario is significantly less than in the dual contaminant scenario (Fig. 4). This is expected because TCE consumption does not aid in biomass growth and because the toxic product formation from TCE degradation results in increased biomass decay. When TCE exists as the single solute and at low M_o, the TCE mass is removed at rates only slightly less than those of the dual solute scenario at low M_o. For the TCE-only scenario at high M_o, however, the biomass is depleted before any substantial amount of degradation can occur (Fig. 4, all plots).

The relative effect that the presence of a co-solute has on mass removal also depends on the biodegradation rate. Simulations using the bslowQbiodegradation parameters tend to accentuate co-solute effects for the degradation of toluene, but suppress differences for TCE. Slower TCE degradation allows TCE to persist and continue to inhibit the toluene degradation for a longer duration than in the bfastQdegradation cases. Conversely, slower toluene biodegradation rates suppress the cometabolic biodegradation rate enhancement of TCE (see Eq. (G) in Table 3).

At both low and high M_o, toluene and TCE mass removals are significantly influenced by the soil type. Greater mass transfer constraints imposed by the Type II soil relative to the Type I soil result in overall 5-day mass reductions for toluene that are several orders of magnitude less for toluene in the Type II soil versus the corresponding scenario in the Type I soil (full dataset not shown in Fig. 3). Likewise, for all TCE scenarios, except TCE at high M_o, mass fractions of